Bachelor Thesis

University of Innsbruck

Precision Measurements of the Higgs Boson with the ATLAS Detector

Author

Felix Dietrich

CERN-THESIS-2016-267
24/05/2016

Insitute for Astro- and Particle Physics
Faculty for Mathematics, Computer Science and Physics
Supervisor: Ao. Univ.-Prof. Emmerich Kneringer

Innsbruck, July 2016

Contents

1 Theory of the Standard Model

The Standard Model of particle physics, as it exists since the late sixties and early seventies, is the most complete theory of particle interactions to this date, even though it only includes three of the four fundamental forces. Experimental discoveries like those of the W and Z bosons in the early eighties [1], the top quark in 1995 [2] and, more recently, the Higgs boson in 2012 [3], have only lent further credence to the theory. While the existence of phenomena like neutrino oscillations strongly indicate that the standard model is not a complete description of fundamental particles, let alone forces, it remains the best theoretical description within its limits, as possible extensions to the standard model still lack general experimental evidence. The goal of this section is obviously not to give a recount of the established theoretical content, but to show some qualitative insights into the more subtle aspects of the theory, which eventually lead to the need for the Higgs particle. Even if someone were to accept quantum field theory and the standard model as the ultimate description of reality, this section will not necessarily explain what is actually going on (as this would still go way beyond the scope of this part), but give more of a qualitative overview of how the Higgs mechanism works, and why this theoretical construct is ultimately necessary to give the property of "mass" to fundamental particles.

1.1 Fermions and their masses

We will start by looking at how the Higgs phenomenon ultimately becomes a more obvious or "natural" method to give fundamental fermions their masses, even though the Higgs mechanism was introduced to give masses to gauge bosons. This approach has one important benefit; it will not be necessary to go all the way into the depths of quantum field theory yet. Instead we will start with the relativistic wave equation of half-integer spin particles, the Dirac equation. Using Planck units, the equation Dirac originally wrote down reads

$$i\frac{\partial}{\partial t}\Psi = \left(-i\sum_{n=1}^{3}\alpha_n\frac{\partial}{\partial x^n} + \beta m\right)\Psi, \tag{1.1}$$

with Ψ as a yet to be defined object that is dependent on space and time $\Psi = \Psi(x,t)$ and closely related to the the wave function that results from the Schrödinger equation. We can identify the energy operator $\hat{E} = i\frac{\partial}{\partial t}$ and the three momentum operators $\hat{p}_n = -i\frac{\partial}{\partial x^n}$. To generate the correct relativistic energy-momentum relation,

$$E^2 = p^2 + m^2, \tag{1.2}$$

the objects α_n and β must satisfy

$$\begin{aligned} \{\alpha_i, \alpha_j\} &= 2\delta_{ij} \\ \{\alpha_i, \beta\} &= 0 \\ \beta^2 &= 1 \end{aligned} \tag{1.3}$$

with the curly brackets denoting the anticommutator $\{a, b\} = ab + ba$. The objects α_n and β obviously can't be numbers, but they can be matrices. The smallest matrices that satisfy these relations in three spatial dimensions are 4x4 matrices. This in turn implies that Ψ is a four-component object (actually it is more like two two-component objects, but more on that later). There are multiple ways to create such matrices; the way used here (adopted from [4]) differs from the one usually chosen in textbooks, but gives insight to one subtle property of the Dirac equation that is often only glanced at or even completely overlooked. Without going into further detail, the matrices are written as

$$\alpha_1 = \begin{pmatrix} 0 & -1 & 0 & 0 \\ -1 & 0 & 0 & 0 \\ 0 & 0 & 0 & 1 \\ 0 & 0 & 1 & 0 \end{pmatrix} \alpha_2 = \begin{pmatrix} 0 & i & 0 & 0 \\ -i & 0 & 0 & 0 \\ 0 & 0 & 0 & -i \\ 0 & 0 & i & 0 \end{pmatrix} \alpha_3 = \begin{pmatrix} -1 & 0 & 0 & 0 \\ 0 & 1 & 0 & 0 \\ 0 & 0 & 1 & 0 \\ 0 & 0 & 0 & -1 \end{pmatrix} \beta = \begin{pmatrix} 0 & 0 & 1 & 0 \\ 0 & 0 & 0 & 1 \\ 1 & 0 & 0 & 0 \\ 0 & 1 & 0 & 0 \end{pmatrix} \tag{1.4}$$

or, in a more elegant form using the Pauli spin matrices σ_i and the 2x2 unit matrix I

$$\alpha_i = \begin{pmatrix} -\sigma_i & 0 \\ 0 & \sigma_i \end{pmatrix} \quad \beta = \begin{pmatrix} 0 & I \\ I & 0 \end{pmatrix}. \tag{1.5}$$

It is easy to verify that these matrices satisfy the relations in (1.3). By writing α and β this way, often called the Weyl or chiral representation, we will conveniently get some insight about the mass term m.[1] In the absence of mass, the first two components of Ψ and the last two are independent, motivating the notation

$$\Psi = \begin{pmatrix} \Psi_L \\ \Psi_R \end{pmatrix}. \tag{1.6}$$

These objects are sometimes referred to as Weyl fermions, since they first appeared as the solution to Hermann Weyl's equation for massless spin 1/2 particles. In naive way, they can be thought of as one half of a massive, "Dirac fermion," described by a general solution Ψ to equation (1.1). While they have not been observed as fundamental particles, recent experiments show that they exist as emergent quasiparticles in semimetals [5]. To show how the Weyl representation relates to the more commonly used Dirac representation, we consider a particle of zero momentum. For an ordinary wavefunction, this means that the spacial derivatives are zero. We can thereby simplify (1.1) to two coupled differential equations:

[1] Of course that is not proprietary to this representation, as all ways of writing the matrices are equal. It is however hidden for example in the commonly used Dirac representation.

$$i\frac{\partial}{\partial t}\Psi_L = m\Psi_R \tag{1.7}$$

$$i\frac{\partial}{\partial t}\Psi_R = m\Psi_L \tag{1.8}$$

If we plainly solve this system of equations, we can see that it oscillates with a frequency of m. In a more quantum mechanical way of writing, we can introduce $\Psi_+ = \Psi_L + \Psi_R$ and $\Psi_- = \Psi_L - \Psi_R$ (ignoring any normalisation constants). By adding (1.7) to (1.8) we obtain the uncoupled set of equations

$$i\frac{\partial}{\partial t}\Psi_+ = m\Psi_+ \tag{1.9}$$

$$i\frac{\partial}{\partial t}\Psi_- = -m\Psi_-. \tag{1.10}$$

We still have not really defined what Ψ actually is, but the objects Ψ_+ and Ψ_- can be interpreted as energy eigenstates of the Dirac equation (when interpreted as a Schrödinger equation) and we can see that one has a positive and the other one a negative energy eigenvalue. Even if we had included the momentum terms, these negative energy values cannot be eliminated and ultimately lead to the introduction of antiparticles. This fact would have been immediately obvious in the Dirac representation, while it is somewhat hidden in the Weyl representation. However, this is just a side note for what we care about. The interesting observation is, that the energy eigenstate of the free particle at rest, and thus the mass eigenstate, is a linear combination of the states Ψ_L and Ψ_R. This means that a massive fermion can be thought of as a superposition of two fundamental states. Before we elaborate on what these states are, we will switch to the modern form of notation by introducing a new way of writing the Dirac matrices:

$$\gamma^0 = \beta \quad \text{and} \quad \gamma^i = \beta\alpha_i, \tag{1.11}$$

These matrices are often called the contravariant gamma matrices. They allow us to write the Dirac equation in a more elegant way, highlighting its relativistic invariance. By multiplying both sides of (1.1) with β and using (1.11) we get the covariant form of the Dirac equation

$$(i\gamma^\mu\partial_\mu - m)\Psi = 0 \tag{1.12}$$

In addition to the four γ-matrices defined above, there is a fifth matrix, usually labelled γ^5, that is defined using the other matrices. It turns out to be diagonal in the Weyl representation

$$\gamma^5 = i\gamma^0\gamma^1\gamma^2\gamma^3 = \begin{pmatrix} -I & 0 \\ 0 & I \end{pmatrix}, \tag{1.13}$$

showing why why chose this set of matrices in the first place. Without going too much into detail, γ^5 is called the chirality operator. Its eigenvalues correspond to left-handed

and right-handedness, and in the Weyl-basis we can see that the chiral eigenstates are the first two and the last two components of Ψ, which have been defined above as Ψ_L and Ψ_R. From the fully written out and slightly rearranged Dirac equation system,

$$i\partial_t \Psi_L - \sigma \nabla \Psi_L = m\Psi_R \tag{1.14}$$

$$i\partial_t \Psi_R + \sigma \nabla \Psi_R = m\Psi_L, \tag{1.15}$$

it can be seen that for a massless particle ($m = 0$), chirality is conserved. In this case, chirality would be the same as helicity, the projection of spin onto the direction of motion. But unlike helicity, chirality is Lorentz-invariant even for massive particles. Furthermore, as one would assume from what has been established before, the chirality operator γ^5, unlike the helicity operator, does not commute with the Dirac Hamiltonian, which, by Ehrenfest's theorem, also means that chirality can not be conserved with time.

1.2 Chirality, mass and the Higgs

The concept of chirality is of importance in the theory of weak interactions, since the left and right-handed components of Ψ couple differently to the gauge bosons of the weak interaction. Especially the W-Bosons only couple to left-handed fermions and right handed anti-fermions. This can be interpreted with only the left handed fermions carrying the relevant "charge". For simplicity we will assume here that they are charged under U(1), which is of course not true,[2] but will give plenty of insight without going into the details of groups and gauge symmetries. With only the left-handed fermion carrying a charge, the components of Ψ would transform like

$$\begin{aligned} \Psi_L &\to e^{i\theta}\Psi_L \\ \Psi_R &\to \Psi_R \end{aligned} \tag{1.16}$$

with a constant, denoted by θ, and $e^{i\theta}$ as the generator of U(1). The symmetry is broken by the mass term in (1.14) and (1.15), as either the right hand side or the left hand side picks up a complex phase under the transformation. To compensate for this, a new complex scalar object Φ is introduced. As a complex field, it could carry charge under U(1), meaning

$$\Phi \to e^{i\theta}\Phi. \tag{1.17}$$

By replacing the mass term with this new field Φ and a coupling constant g, we now can create an explicitly gauge invariant formalism:

$$i\partial_t \Psi_L - \sigma \nabla \Psi_L = g\Phi\Psi_R \tag{1.18}$$

$$i\partial_t \Psi_R + \sigma \nabla \Psi_R = g\Phi^*\Psi_L, \tag{1.19}$$

In order for Ψ to become massive, Φ has to assume a non zero value in the vacuum.[3]

[2] As SU(2) is the symmetry group of the weak force.
[3] This will be examined more closely in section 1.3.

Before going further, we will introduce the Dirac adjoint, $\bar{\Psi} = \Psi^\dagger \gamma_0$. By multiplying it on both sides of the Dirac equation, we can construct the Dirac-Lagrangian:

$$\mathcal{L}_{Dirac} = i\bar{\Psi}\gamma^\mu \partial_\mu \Psi - m\bar{\Psi}\Psi \tag{1.20}$$

By looking at the "mass" term in the Lagrangian, and its replacement with the field Φ and a coupling constant,

$$m\bar{\Psi}\Psi = m(\Psi_L^\dagger \Psi_R + \Psi_R^\dagger \Psi_L) = g(\Psi_L^\dagger \Phi \Psi_R + \Psi_R^\dagger \Phi^* \Psi_L), \tag{1.21}$$

we can draw a diagram of the interaction:

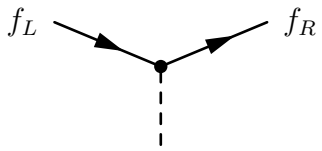

Figure 1.1: Diagram for the mass term in the Lagrangian. The chiral fermion interacts with the vacuum expectation value of the scalar field, turning it from left-handed to right-handed. Charge conservation is no longer violated when changing from left-handed to right-handed, as the charges can be exchanged with the field Φ.

In addition to the non-zero vacuum expectation value, there is another peculiar property of the field Φ. Without going into detail, there is a degree of freedom to the field that corresponds to a massive excitation H. Acknowledging this, Φ can be written as

$$\Phi = v + H. \tag{1.22}$$

Using this expression, (1.21) becomes

$$m\bar{\Psi}\Psi = gv(\Psi_L^\dagger \Psi_R + \Psi_R^\dagger \Psi_L) \tag{1.23}$$

$$+ gH(\Psi_L^\dagger \Psi_R + \Psi_R^\dagger \Psi_L) \tag{1.24}$$

The mass of Ψ is given by its coupling constant and the vacuum expectation value of Φ:

$$m = gv, \tag{1.25}$$

but there is also a chance to create an excitation H. The field Φ corresponds to the Higgs Field and the massive excitation H to the Higgs Boson.

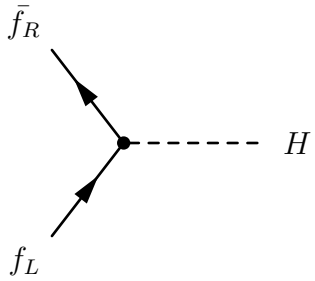

Figure 1.2: Diagram for the creation of a Higgs boson from a fermion/anti-fermion pair.

The expectation value v for the Higgs field was experimentally established to be around 245 GeV. Every fermion's mass is now determined by its Yukawa coupling constant g, which is $\approx 10^{-6}$ for the electron. For the most massive quark, the top quark, it is close to unity. The coupling constant g can be interpreted as the probability of the interaction, meaning that figure 1.2 is much more likely to happen for a top/anti-top quark pair than for an electron/positron pair. This means that in order to produce a significant amount of Higgs bosons, one needs to be able to produce a lot of of top quarks. To this day, the only hadron colliders powerful enough to produce top quarks are the Tevatron at Fermilab and the Large Hadron Collider at CERN. The way this usually happens in those colliders is shown in figure 2.1.

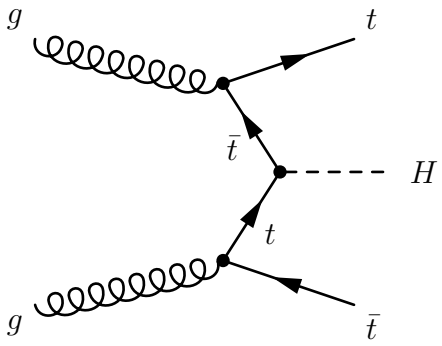

Figure 1.3: Feynman-Diagram for the creation of a Higgs boson through top/anti-top fusion. This is the most simple way of creating a Higgs boson in relation to figure 1.2, but not the most common one utilized in hadron colliders.

By looking at the Lagrangian, we can also deduce ways in which the Higgs boson might decay. In general, the Higgs will decay into heavier fermions since their coupling is stronger. The exact branching ratios however are heavily dependent on the actual mass of the Higgs, which remains a free parameter of the theory and hinders specific experimental searches.

1.3 The masses of gauge bosons

The fundamental forces are described by the exchange of vector particles, which arise from the quantisation of vector fields. The corresponding bosons are the photon for the electromagnetic force, the eight gluons for the strong force and the W and Z bosons for the weak force. The photon and the gluons are massless, but weak bosons have masses of 80,4 GeV/c^2 and 91,2 GeV/c^2 respectively. However, the gauge bosons cannot have masses by themselves. In order for them to be massive, the Higgs mechanism is introduced. This section intends to give some basic insight on why that is the case, as a complete discussion would once again go way beyond the scope of this chapter.

For simplification, just as in the last section, we will look at a case where the photon has its symmetry spontaneously broken, this time giving the gauge boson itself mass in the process. A relativistic vector field is described by a four-vector A^μ, which for the electromagnetic field corresponds to the four-potential made up of the electric potential and the magnetic vector potential. The four-potential cannot be directly observed, unlike the associated field strengths, which are found in the components of the electromagnetic field tensor

$$F^{\mu\nu} = \partial^\mu A^\nu - \partial^\nu A^\mu. \tag{1.26}$$

Ignoring the details of its construction, the Lagrangian for a free, massive photon field would look like

$$\mathcal{L} = -\frac{1}{4} F_{\mu\nu} F^{\mu\nu} - \frac{1}{2} m^2 A_\mu A^\mu. \tag{1.27}$$

The mass enters as the square of the gauge boson mass m and is quadratic in the field. Under a gauge transformation

$$A_\mu^{'} = A_\mu + \partial_\mu \theta \tag{1.28}$$

the field tensor term of the Lagrangian remains unchanged. But the mass term obviously breaks the gauge symmetry, so it cannot simply be added to the Lagrangian in this form. Something akin to a mass term can only be introduced by adding a new scalar field that interacts with the gauge boson. The Lagrangian of a free complex scalar field Φ can be constructed as follows:

$$\mathcal{L} = \partial^\mu \Phi^* \cdot \partial_\mu \Phi - \mu \Phi^* \Phi - \lambda (\Phi^* \Phi)^2 \tag{1.29}$$

The last two terms can be interpreted as the potential

$$V(\Phi^* \Phi) = \mu \Phi^* \Phi + \lambda (\Phi^* \Phi)^2 \tag{1.30}$$

of the Field. For a negative value of μ, spontaneous symmetry breaking occurs and the potential assumes the frequently referenced form of a mexican hat. The radial symmetry motivates writing the field in polar coordinates:

$$\Phi = \rho e^{i\alpha} \tag{1.31}$$

with ρ as the distance from the origin and α as the phase angle of the field. In the case of spontaneous symmetry braking, the potential no longer has just one minimum, but an infinite amount on a circle around the origin of the complex plane

$$\Phi_0 = \sqrt{\frac{\mu}{2\lambda}} e^{i\alpha}, \tag{1.32}$$

only distinguished by the phase angle. In this case there are two possible excitations: One radial and one angular. The angular one would correspond to a massless Goldstone boson and the radial one to a massive Higgs boson. To emphasize this, we could rewrite the Lagrangian in terms of two scalar fields σ and η

$$\Phi = \frac{1}{\sqrt{2}}(v + \sigma + i\eta) \tag{1.33}$$

and one would immediately see that σ picks up a mass term of $\sqrt{2\lambda}$ and η doesn't get any mass term. However, we are more interested in how the mechanism gives mass to the gauge boson. By introducing the covariant derivative

$$D = \partial_\mu + igA_\mu \tag{1.34}$$

which includes the gauge field and a coupling constant g, we can construct a Lagrangian that is also invariant under the local gauge transformations

$$\begin{aligned} \Phi' &= e^{i\theta(x)}\Phi \\ A_\mu &= A_\mu + g^{-1}\partial_\mu\theta(x) \end{aligned}$$

and takes the form

$$\mathcal{L} = D\Phi^* D\Phi + V(\Phi^*\Phi) - \frac{1}{4}F_{\mu\nu}F^{\mu\nu}. \tag{1.35}$$

By assuming that the radial component of Φ, ρ, is basically constant at a value of v,

$$\Phi = v \cdot e^{i\alpha} \tag{1.36}$$

the covariant derivative factor is only left with derivatives of α.

$$D\Phi = ve^{i\alpha} i(\partial_\mu\alpha + gA_\mu) \tag{1.37}$$

Now we can make a gauge transformation with $\theta = -\alpha$ in order to absorb the α-derivatives into A_μ. The product of the covariant derivatives will only leave a term in the Lagrangian that looks like

$$g^2 v^2 A_\mu A^\mu. \tag{1.38}$$

This is precisely the form of a mass term for the gauge boson (1.27), only with m being replaced by gv. The Goldstone boson has disappeared, it was "eaten" by the now massive gauge boson.

In this model, the photon would now have gained a mass along with a third, longitudinal degree of freedom, next to the two transversal degrees of freedom, that are usually defined by its polarisation. Being massive, it would limit the range of the electromagnetic force. As a side note, it should be mentioned that while the photon usually doesn't have its symmetry spontaneously broken, this is very similar to what happens in the Ginzburg–Landau theory of superconductors, explaining the Meissner effect, where magnetic field lines can no longer penetrate a superconductor below the critical temperature.

In the standard model of particle physics, the Higgs mechanism gives mass to the weak W and Z bosons. By looking at the coupling of the Higgs to the gauge bosons in the Lagrangian, we can illustrate the processes pretty much in the same way as in section 1.2.

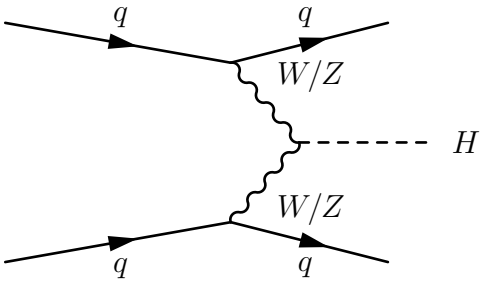

Figure 1.4: Feynman-Diagram for the creation of a Higgs boson from two weak bosons. Concurrently, the inverse can also be a way for the Higgs to decay.

The concept itself, nowadays commonly referred to as the Higgs mechanism, was first introduced by Paul Anderson in 1962 [6] and fully worked out for the first time two years later by three independent groups: Robert Brout and François Englert [7], Peter Higgs [8], and the group of Gerald Guralnik, Carl Richard Hagen, and Tom Kibble [9]. Higgs and Englert were awarded the 2013 Nobel Prize in Physics for their contributions.

2 Experimental search and discovery of the Higgs boson

For a long time, the Higgs boson remained the only unobserved fundamental particle of the Standard Model, giving substantial motivation to the experimental search for it. Ellis et al. [10] give a recount of events until 2012. After the first studies of possibilities regarding production and decay of the Higgs boson in the early seventies, the range the Higgs mass remained very uncertain. First estimations regarding a Higgs that weighed up to 100 GeV/c^2 basically concluded that there was no reasonable way to find it experimentally. In 1975 a study [11] concluded with discouraging experimental search, for "having no idea what is the mass of the Higgs boson" and "for not being sure of its couplings to other particles, except that they are probably all very small".

2.1 Searches at the LEP collider

By 1976, early discussions surfaced on searching the Higgs boson in e^+e^- collisions [12]. They concluded that there are three important processes for producing the Higgs boson at a collider like the LEP (Large Electron Positron Collider):

$$\begin{aligned} Z &\to H + f\bar{f} \\ e^+e^- &\to Z + H \\ e^+e^- &\to \nu H\bar{\nu} \text{ or } e^+He^- \end{aligned}$$

The productions are via Z-decay, in association with the Z and via W^+W^- or ZZ fusion. The direct process $e^+e^- \to H$ is negligible because of the extremely small coupling, as described in section 1.2. For a muon collider, this reaction could be more important. Unfortunately, no such collider has made it beyond the planning phase so far.

After the start of operations in 1989, LEP was able to accelerate electrons and positrons up to a total energy of 45 GeV each, enabling the production of Z-bosons. The high precision data on electroweak interactions gained from this collider, allowed useful estimates of the Higgs mass m_H for the first time. First estimates already placed m_H in the area below 300 GeV/c^2 and above 58 GeV/c^2, but the discoveries and precise measurement like that of the top quark allowed a first accurate range constraint for the Higgs mass:

$$m_H \approx 100 \pm 30 \text{ GeV/c}^2$$

With successive upgrades at the LEP, reaching a center of mass energy of up to 206 GeV at the final LEP 2 runs, the lower limit for m_H was constantly pushed up further. Unfortunately, LEP 2 had reached its limits in the year 2000 and was consequently shut down and dismantled to make room for the new Large Hadron Collider, the LHC. From there on, the lower limit for the Higgs mass remained at 114 GeV/c^2 at a 95% confidence level [24].

2.2 Searches at the LHC

Experiments at the Large Hadron Collider began in the year 2009. The collider uses the same 26 km circumference tunnel that the LEP used before its operation ended. After problems at the beginning, the LHC reached its first intended center of mass energy of 7 TeV in 2010 and continued experiments until the end of 2012, when it entered a new phase of upgrading. During this phase, the discovery of a new particle, in concordance with the Higgs at a mass of ≈ 126 GeV/c^2, was officially announced [3].

2.2.1 Production

In general, a hadron collider like the LHC poses more problems when it comes to producing Higgs bosons than an e^+e^- collider like the LEP, because particles like the proton and the neutrons are not fundamental particles. Collisions at the LHC produce a large background, while at the same time Higgs-production via quark constituents is small because of their low masses. There is however an additional, prolific possibility: The production by gluon-gluon fusion via a triangle loop [13]. While this is the dominant way of production at the LHC, there are also other possibilities. One is the production via Higgs-strahlung in association with $W^\pm$ or Z bosons. The third important process is by W^+W^- and ZZ fusion. All of those diagrams are shown in figures 2.1 to 2.2.

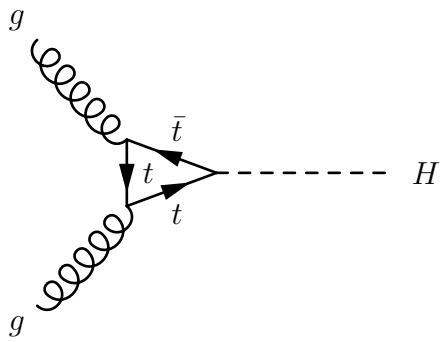

Figure 2.1: Feynman-Diagram for the creation of a Higgs boson through a top-quark loop (also referred to as gluon-gluon fusion). In an even more complete diagram, the gluons themselves would originate from quarks. This is the most prevalent way to create a Higgs boson at the LHC.

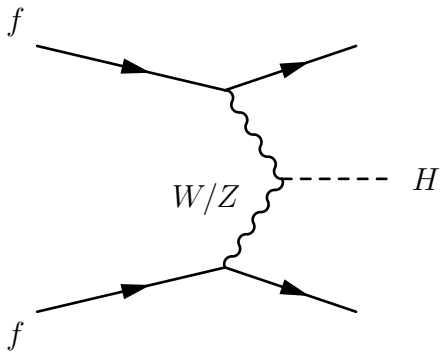

Figure 2.2: Production of a Higgs boson by weak vector-boson fusion. The two fermions can be of a different type. They exchange virtual W or Z bosons, which in turn can emit a Higgs boson. This was the second most important method of production at the LEP and currently is the second best at the LHC.

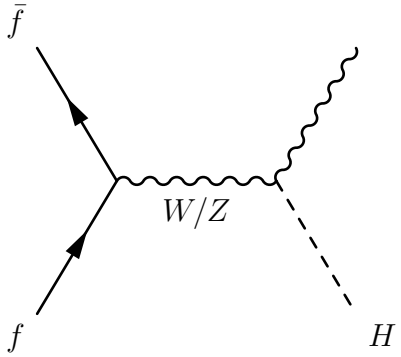

Figure 2.3: Production of a Higgs boson by Higgs-strahlung. A fermion/antifermion pair collision can produce a virtual W or Z boson, which in turn can emit a Higgs boson. This was the most important way of producing Higgs bosons at the LEP and currently is the third most important way at the LHC.

2.2.2 Decay

The production of the Higgs boson is only the first part of the experimental search. The second, even more important part is actually finding it through its possible decays. Generally, the decay of the Higgs principally works much like the production. In practice however, the branching ratios of the various decay channels are heavily dependent on m_H. As shown in figure 2.4, which depicts results computed and published by the LHC Higgs Cross Section Working group in 2013, in the relevant mass region around 125 GeV/c^2, the dominant decay product of the Higgs is a pair of bottom quarks. The bottom's mass of roughly 4.2 GeV/c^2 is much smaller than that of the top quark at approximately 172 GeV/c^2, meaning its coupling is much smaller as well. But at $m_H \approx 125$ GeV/c^2, the top decay is heavily suppressed because the Higgs simply isn't massive enough to produce a top pair. The decay into top quarks only becomes important when $m_H \approx 350$ GeV/c^2, which is roughly twice the mass of the top quark, as shown on the right in figure 2.4.

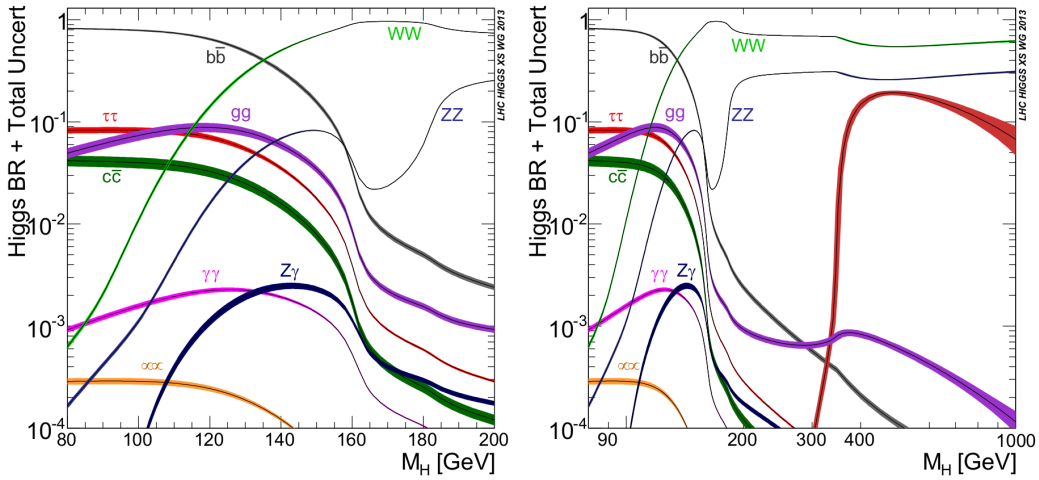

Figure 2.4: Branching ratios including uncertainties for the low mass range (left) and for the full mass range (right) of the Higgs. Source: [14], page 5.

When it comes to finding signals from the decay of a Higgs boson, the quark antiquark decays are not accessible anyways. The most important decays for the discovery of the Higgs are decays into two photons and decays into four leptons via a ZZ pair (one of those being virtual).

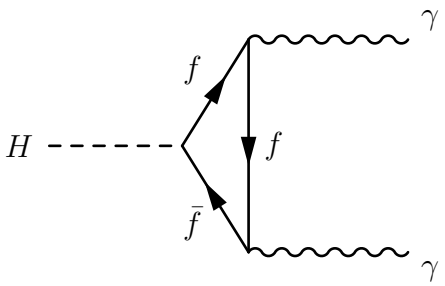

Figure 2.5: Feynman-Diagram for the decay of a Higgs boson into two photons via a quark loop. This is one of the two ways by which the Higgs boson originally was discovered.

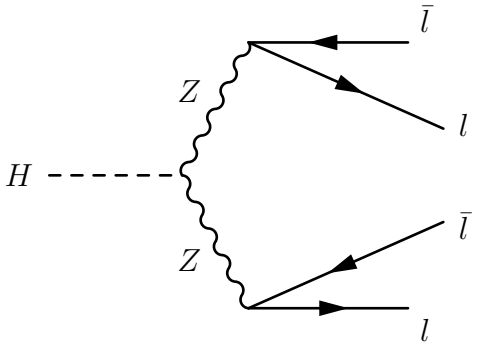

Figure 2.6: Decay of a Higgs boson into two photons via Z bosons. This is the second way by which the Higgs was first discovered at the LHC.

The two photon branching ratio at $m_H \approx 125$ GeV/c^2 is comparatively low ($\gamma\gamma$ line in figure 2.4), resulting in the need for a lot of data to conclusively verify or dismiss any signal.

2.2.3 The ATLAS detector

Production of the Higgs boson alone is not sufficient for its discovery, it also requires a detector in order to study decay products. The ATLAS detector is one of seven detectors at the LHC and one of the two detectors to eventually find conclusive evidence for the Higgs. It is comprised of two large superconducting magnet systems and three main detector parts, installed in a toroidal shape around the LHC beam tube. Two 6.3 cm beam pipes inside the LHC tube covey proton (or heavy ion) beams in opposite directions inside an ultra high vacuum environment. The inner detector, starting a few centimetres from the beam axis, consists of three parts: The innermost silicon based Pixel Detector, with a very high resolution (approximately 50x400 micrometers), the Semi-Conductor-Tracker which is similar to the Pixel Detector albeit with lower resolution and the outer Transition Raidation Tracker, which contains straws filled with gas that becomes ionized when a particle passes through. With the information from these detectors the starting points of particles can be identified, for example to see if multiple particles originate from the same location. It also provides information about the track of the particle as it passes through the detector. Trajectories of charged particles are bent by 2 T magnetic fields, allowing the particle's momentum to be measured.

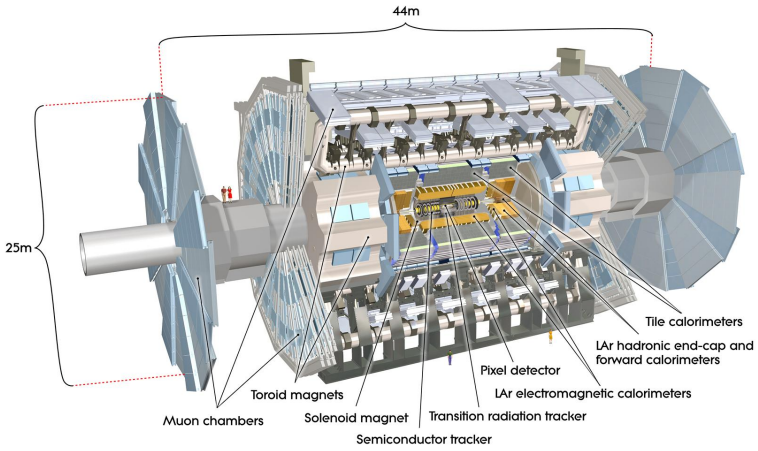

Figure 2.7: View of the ATLAS detector structure. The LHC beam pipes pass through horizontally, intersecting in the middle of the detector. Source: J. Pequenao, ATLAS Experiment, 2008

Outside the solenoid magnets surrounding the inner detector, two calorimeters are installed. The electromagnetic calorimeter measures the energy of charged particles when they are absorbed in a high density metal (mostly lead and stainless steal), producing a

particle shower. The outer hadronic calorimeter measures particles that interact through the strong force, i.e. primarily hadrons. The EM calorimeter can measure a particles pseudorapidity (basically a measure of its angle relative to the beam axis) to within 1.5 degrees, and the hadronic calorimeter can measure it within 6 degrees. The outermost part of the detector, the muon spectrometer, is solely designed to detect muons, after they pass through all other detectors. Like the inner detector, it uses a system of strong magnets to measure the muon momentum from the curvature of its path through the detector.

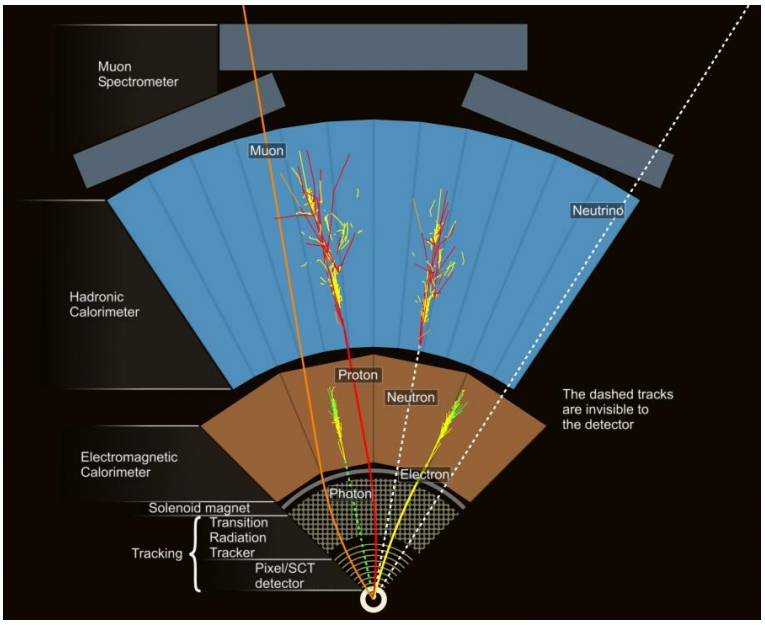

Figure 2.8: Schematic detection of different particles inside the ATLAS detector. Note that a neutrino, shown as a white dotted line, can not directly be detected. Source: J. Pequenao, ATLAS Experiment, 2008

The detector produces a large amount of data, necessitating filters to enable transfer and storage of events. A trigger system directly built into the electronics and selects roughly 100,000 events out of several million every second. Two additional trigger systems run on nearby computer clusters, eventually leaving several hundred events per second to be stored and processed further [17] [18].

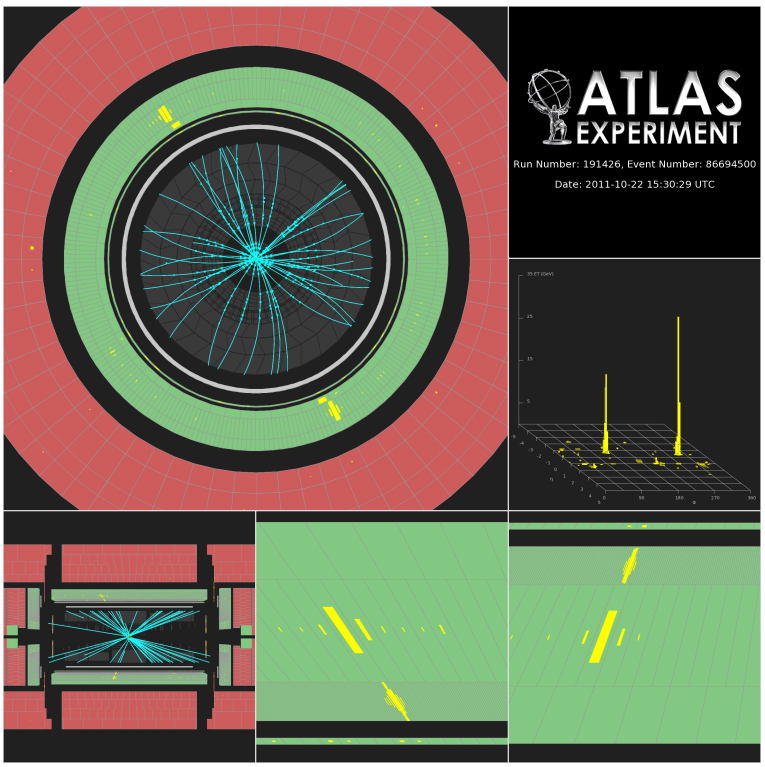

Figure 2.9: Visualisation of a Higgs candidate $\gamma\gamma$-event recorded at Atlas in 2011. The top image shows a cross section of the detector viewed parallel to the beam tube, the bottom left image a perpendicular view. The photons (yellow peaks) are absorbed in the EM calorimeter (green area), but they leave no trace in the inner detector (gray area with blue lines), allowing to differentiate them from e.g. electrons. Source: ATLAS Experiment

2.2.4 Initial results

After some preliminary reports that indicated the possible discovery of a new particle in the suspected Higgs mass region, the ATLAS and CMS detector groups published results showing conclusive evidence for a new boson. The ATLAS group detected the particle at 126 GeV/c^2 at a significance of 5.9 standard deviations and the CMS group at 125 GeV/c^2 with a significance of 5 standard deviations. The distribution of invariant mass of $\gamma\gamma$ events recorded at the ATLAS experiment (figure 2.10), shows an excess of such events in the 126 GeV/c^2 area.

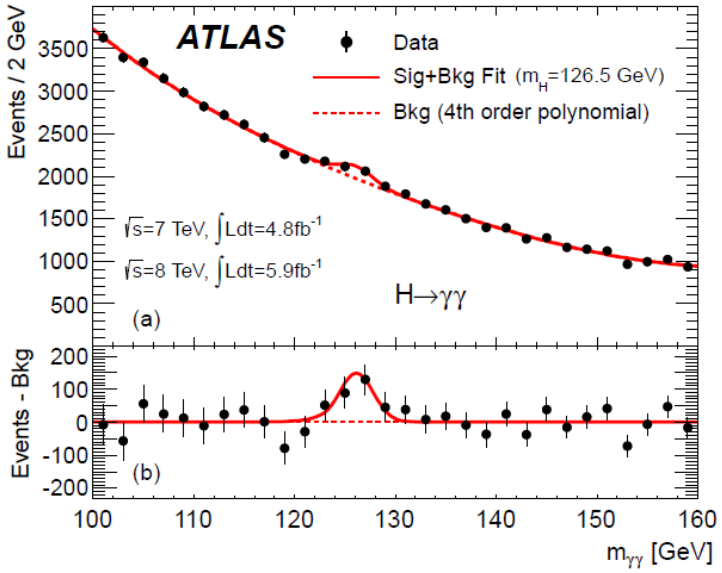

Figure 2.10: Invariant mass distribution of $\gamma\gamma$ events from the ATLAS experiment. Shown in red is a fit to the data of a signal component fixed to $m_H = 126.5$ GeV/c^2. The background is described by a fourth order polynomial and represented by the dashed red line. Source: [15], page 10.

A signal was also found in other channels, most importantly where the Higgs decays into two W bosons (one of them virtual) and results in two oppositely charged leptons and two neutrinos, manifesting in a large momentum imbalance between the leptons. The decay channel via two Z bosons (also one virtual) decaying into four leptons also showed a signal. The strength of the respective signals, with $\mu = 1$ representing the standard model Higgs boson, is shown in figure 2.11, together with the combined signal strength which raised the significance above the necessary 5 sigma value for the discovery. This represents enough evidence to justify the discovery of a new particle at a mass of approximately 126 GeV/c^2

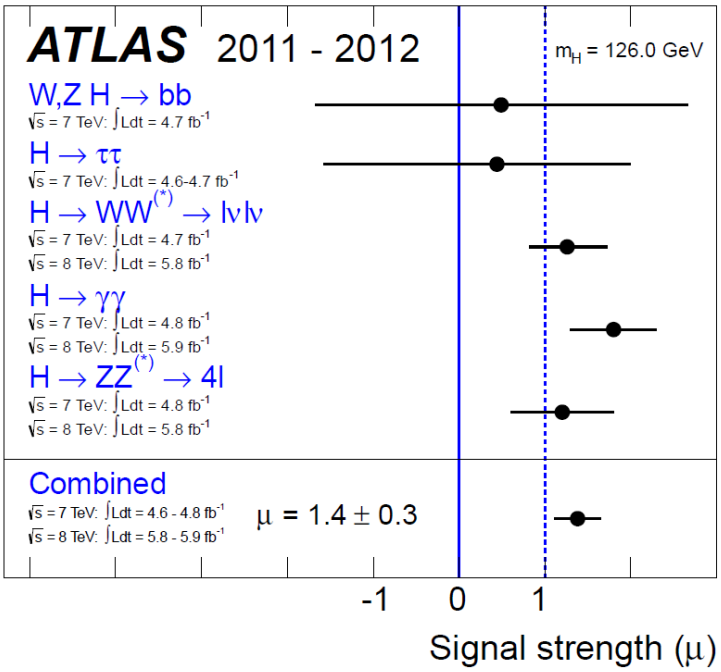

Figure 2.11: Signal strength parameter μ of the respective channels for $m_H = 126$ GeV/c^2 and the combined value $\mu = 1.4 \pm 0.3$ for the Standard Model Higgs hypothesis ($\mu = 1$). Source: [15], page 19.

3 Precision measurements and Standard Model tests

While the decay channels that enabled the original discovery already fit theoretical predictions, the question remained whether or not the new particle at $126\,\mathrm{GeV/c^2}$ also exhibited other properties of the Higgs. This chapter will analyse several of those properties and combine more recent experimental results in order to conclude that the new particle is in fact the Standard Model Higgs boson.

3.1 Branching ratios

At first we examine if the measured decay rates actually fit the theoretical predictions. Theoretical values on different Standard Model Higgs branching ratios and decay widths are published by CERN online [19]. In order to verify on some of those values, the high energy particle collision event simulation program PYTHIA is used here. Originally written in FORTRAN, it was eventually ported to C++ and is developed and maintained by Torbjörn Sjöstrand, Stefan Ask, Richard Corke, Stephen Mrenna, Stefan Prestel, and Peter Skands. According to the developers, it "*contains theory and models for a number of physics aspects, including hard and soft interactions, parton distributions, initial- and final-state parton showers, multiparton interactions, fragmentation and decay. It is largely based on original research, but also borrows many formulae and other knowledge from the literature.*"

The program was used to simulate the decay of a Higgs boson assuming standard model physics. As the Higgs mass is a free parameter of the standard model, one can pass it to the generator in order to simulate the decays for different Higgs masses while keeping everything else constant, allowing to study the decay branching ratio behaviours. The evaluated data from 2 example simulation runs, each one simulating 1000 Higgs decays, one at a mass of $125\,\mathrm{GeV/c^2}$ and one at $400\,\mathrm{GeV/c^2}$, are shown in tables 3.1 and 3.2. The percentages gained from the simulations are within 2% of the percentages published in [19] and shown collectively in figure 2.4.

Decay	Nr. observed	Percentage
bb	577	58
WW^*	215	22
gg	84	8
$\tau\bar{\tau}$	64	6
ZZ^*	31	3
$c\bar{c}$	23	2
$\gamma\gamma$	5	0.5
γZ	1	0.1

Table 3.1: Simulation results of 1000 125 $\mathrm{GeV/c^2}$ SM Higgs decays. Note that only five out of 1000 Higgs particles decayed into two photons, representing one of the channels used in the original discovery depicted in figure 2.10.

Decay	Nr. observed	Percentage
WW	602	60
ZZ	303	30
$t\bar{t}$	94	9
gg	1	0.1

Table 3.2: Simulation results of 1000 400 $\mathrm{GeV/c^2}$ SM Higgs decays. Note that at this mass, the Higgs can decay into two W or Z-bosons, whereas at 125 $\mathrm{GeV/c^2}$ one actually turns out to be virtual, implied by a much lower mass in the simulation output data.

With the data collected from subsequent LHC runs, signals of the Higgs also became evident in many other channels. The results from runs one and two are displayed in figure 3.1, where the 125.36 $\mathrm{GeV/c^2}$ Standard Model Higgs boson corresponds to a signal strength of 1. The one sigma uncertainties are still relatively large in the rarer channels, but the overall results are in line with the theoretical predictions. Only the overall Z-boson channel displays a signal strength slightly more than one standard deviation above the expected value. Also noteworthy, the overall b-quark channel shows a signal strength a little more one standard deviation below the theoretical prediction. Further experimental data will be needed to verify if this behaviour is due to new physics, possibly beyond the standard model, or due to statistical fluctuations.

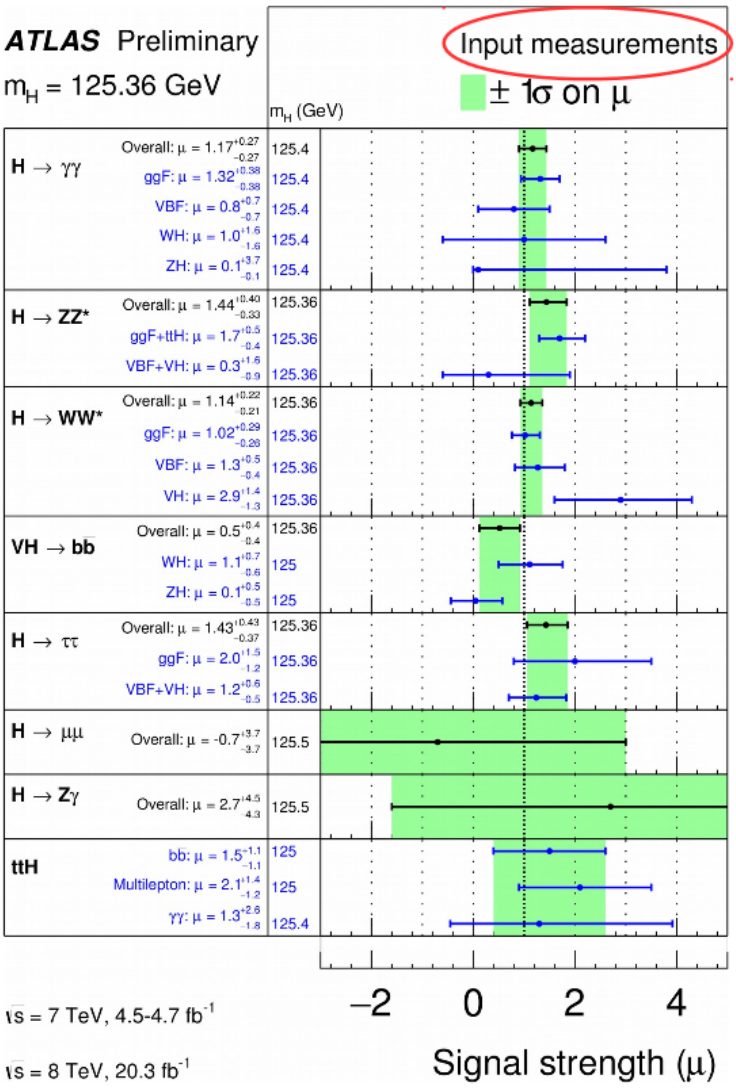

Figure 3.1: Measured Higgs signal strength in various decay channels measured with the ATLAS detector. A signal strength of $\mu = 1$ corresponds to the Standard Model Higgs boson. It can be seen that uncertainties are still very large in some branches, e.g. for the rare $Z\gamma$ decay. Source: ATLAS collaboration

3.2 Spin and parity

As explained in chapter 1, the Higgs field Φ is a scalar field, meaning it is spin 0. This raises the question, whether the new particle at 125 GeV/c^2 also shows spin 0 behaviour. Because of the observed two photon decay, one can exclude the possibility of spin 1, since a massive spin 1 particle cannot decay into two identical massless spin 1 particles [20]. The next step would be discerning between spin 0 and spin 2. Data collected at ATLAS showed that the spin 2 as well as the negative parity hypothesis can be excluded at

the 99.9% confidence level [21]. This conclusion is based on careful analysis of the two-photon and four-lepton decay properties. The the angle Θ^* between the photons and the z-axis of the Collins-Soper frame (see [22]) can be probed for the spin hypothesis. Figure 3.2 shows the results of those tests.

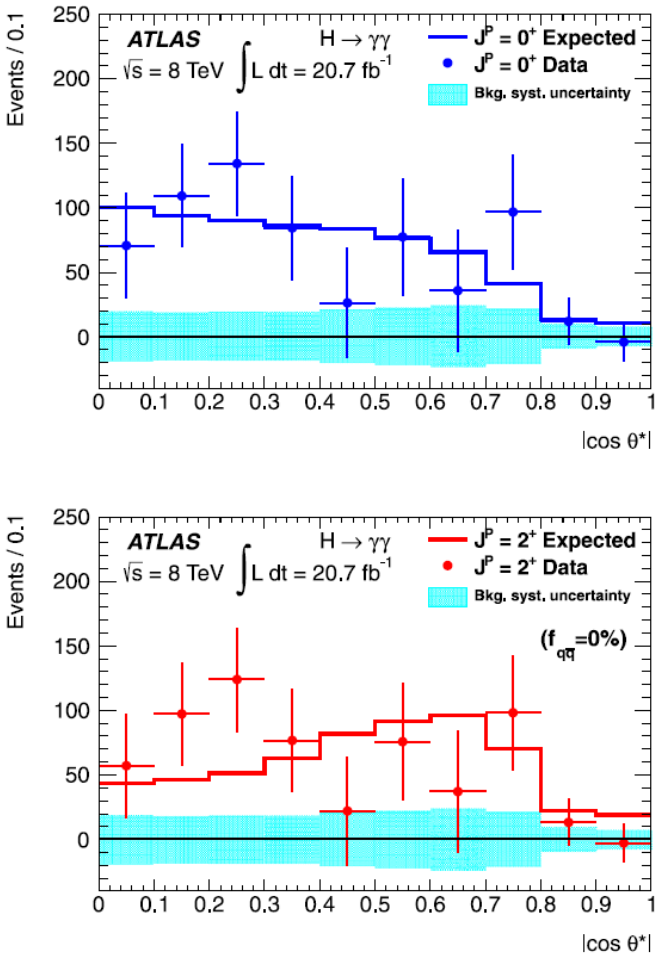

Figure 3.2: Distribution models of $|\cos\Theta^*|$ assuming spin 0 (top) and spin 2 (bottom) with measured data points. Note that the data points were selected differently for the hypothesis tests, meaning that the data points are slightly different even though they appear to originate from the same set. Source: [21]

The $H \to \gamma\gamma$ analysis alone already excludes spin 2 at a confidence level of more than 99%. The four lepton decay can also be probed for Higgs properties, this time using the angle Θ_1 between the negatively charged lepton in the Z_1 rest frame and the direction of flight of the Z_1 in the four lepton rest frame. The masses of the other two leptons is designated as m_{34} and also probed for spin/parity analysis. The selected events can then be compared to the + and - parity hypotheses. The relevant part of the results is

shown in figure 3.3.
Together with other tests not detailed here, the analysis concludes that Spin 2 and negative parity for the new particle can both be excluded at a confidence level above 99.9% [21], giving further credence to the hypothesis that the observed boson is in fact the Higgs boson.

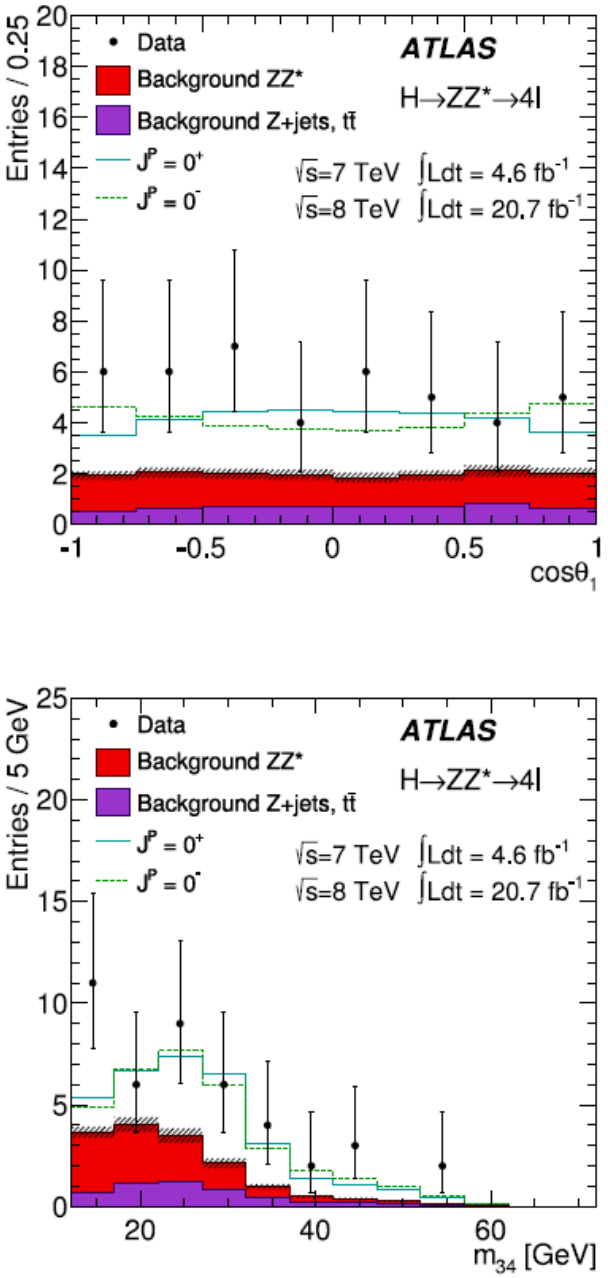

Figure 3.3: Distributions of $\cos\Theta_1$ and m_{34} using selected events from both 7 and 8 TeV run datasets. The solid (dotted) green line shows the contribution from the 0^+ (0^-) hypothesis. Source: [21]

3.3 Coupling to mass

It can be argued that even proving spin 0 is not yet sufficient to call the new particle a Higgs boson [23]. Indeed, the defining quality of the Higgs boson would be its intricate connection to other particle's masses, as outlined in chapter 1. This means that the strength of interactions with other particles should be proportional to their masses. The coupling strength is indeed very much in line with the theoretical prediction. The data gained from all particles is at or very close to the theoretical line shown in figure 3.4. This can be seen as the final piece of the puzzle that allows us to conclude that the particle discovered in 2012 is indeed the Standard Model Higgs boson.

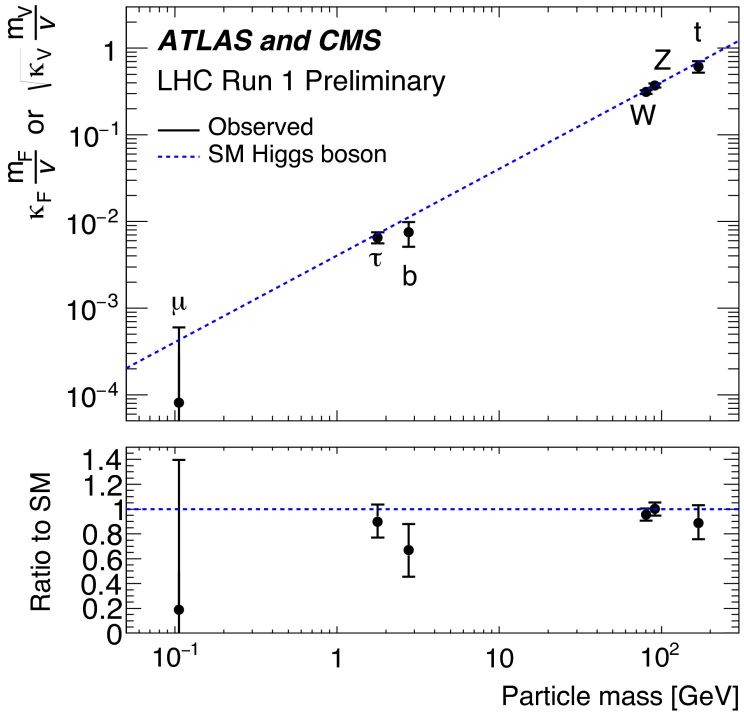

Figure 3.4: Relationship between the strength of the coupling to the Higgs boson and the particles mass for several Standard Model particles. The blue line represents the theoretical prediction that mass is proportional to coupling strength. Compared to fermions, the W and Z bosons have a slightly different relationship to the Higgs boson, which is accounted for in the plot by the square root (see chapter 1). Source: ATLAS and CMS/CERN

4 Summary, conclusion and outlook

We showed how the Higgs mechanism has become a necessary and fundamental part of the Standard Model, giving mass to fundamental fermions and bosons. We briefly described the connections between the Higgs field and the fermion and gauge boson fields, showing how they actually gain mass and how they predict ways to produce the Higgs boson. In the same way, we also studied how the Higgs boson decays, enabling the search for those decay products in particle detectors at the LHC. Additionally, the ATLAS detector was briefly described, showing how particles are detected in different parts of the detector. A brief history of the search for the Higgs boson was given at the LHC, that culminated with the initial announcement of the discovery of a new particle in 2012. Building up on the initial results, detailed analysis of combinations of new and old data showed that the newly discovered particle is indeed very likely the Standard Model Higgs boson. That is: a boson with spin 0, positive parity that couples to other particles proportionally to their mass.

While all the current evidence points to the Higgs boson being the Standard Model Higgs boson, more data will eventually show if this statement holds true in all areas. The results at the LHC's full energy of up to 14 TeV need to remain consistent with the current theoretical predictions. If the future actually fails to unravel new peculiarities, it could be seen as a great triumph of the theory that is the Standard Model. But it could also be considered a letdown for all those who hoped the LHC would finally reach an era of new physics, and a backlash for all the theories beyond the Standard Model, some of which predict much more to be found regarding the Higgs phenomenon.

Bibliography

[1] G. Arnison et al. (UA1 Collaboration) (1983), *Experimental observation of isolated large transverse energy electrons with associated missing energy at s=540 GeV/c^2*, Physics Letters B, Volume 122, Issue 1, 24 February 1983, Pages 103-116.

[2] F. Abe et al. (CDF Collaboration) (1995), *Observation of Top Quark Production in pp Collisions with the Collider Detector at Fermilab*, Physical Review Letters 74 (14), 3 April 1995.

[3] G. Aad et al. (ATLAS Collaboration) (2012), emphObservation of a new particle in the search for the Standard Model Higgs boson with the ATLAS detector at the LHC, Physics Letters B, Volume 716, Issue 1, 17 September 2012, Pages 1–29.

[4] M. Peskin and D. Schroeder, *An Introduction To Quantum Field Theory*, ABP, 1995.

[5] S. Xu et al. *Discovery of a Weyl Fermion semimetal and topological Fermi arcs*, Science, 16 July 2015.

[6] P. W. Anderson (1962), *Plasmons, Gauge Invariance, and Mass*. Physical Review 130 (1): 439–442

[7] F. Englert and R. Brout (1964), *Broken Symmetry and the Mass of Gauge Vector Mesons*, Physical Review Letters 13 (9): 321–323.

[8] Peter W. Higgs (1964), *Broken Symmetries and the Masses of Gauge Bosons*, Physical Review Letters 13 (16): 508–509.

[9] G. S. Guralnik, C. R. Hagen, and T. W. B. Kibble (1964), *Global Conservation Laws and Massless Particles*, Physical Review Letters 13 (20): 585–587.

[10] J. Ellis, G.Ellis, M. K. Gaillard and D. V. Nanopoulos, *A Historical Profile of the Higgs Boson*, arXiv:1201.6045, https://cds.cern.ch/record/1420264, 29 January 2012

[11] J. Ellis, M. K. Gaillard and D. V. Nanopoulos, *A phenomenological profile of the Higgs boson*, CERN preprint Nov. 1975, published in Nucl. Phys. B 106 (1976).

[12] J. Ellis and M. K. Gaillard, Theoretical remarks, in L. Camilleri et al., *Physics with very high-energy e^+e^- colliding beams*, CERN report 76-18 (Nov. 1976), pp 21-94.

[13] H. M. Georgi, S. L. Glashow, M. E. Machacek and D. V. Nanopoulos, *Higgs bosons from two gluon annihilation In proton-proton collisions*, Phys. Rev. Lett. 40 (1978) 692.

[14] S. Heinemeyer et al. (LHC Higgs Cross Section Working Group), *Handbook of LHC Higgs Cross Sections: 3. Higgs Properties*, arXiv:1307.1347, CERN, 2013. - 404 p.

[15] G. Aad et al. (ATLAS Collaboration), *Observation of a new particle in the search for the Standard Model Higgs boson with the ATLAS detector at the LHC*, Physics Letters B, Volume 716, Issue 1, 17 September 2012, Pages 1–29.

[16] S. Chatrchyan et al. (CMS Collaboration), *Observation of a new boson at a mass of 125 GeV/c^2 with the CMS experiment at the LHC*, Physics Letters B, Volume 716, Issue 1, 17 September 2012, Pages 30–61.

[17] N. V. Krasnikov; V. A. Matveev, *Physics at LHC*, Physics of Particles and Nuclei 28 (5): 441–470, September 1997.

[18] Official ATLAS website at *http://atlas.cern/discover/detector*, retrieved 10 July 2016.

[19] Handbook of LHC Higgs Cross Sections: 2. Differential Distributions, LHC Crossections Group / SM Higgs Branching Ratios and Total Decay Widths (update in CERN Report4 2016), https://twiki.cern.ch/twiki/bin/view/LHCPhysics/CERNYellowReportPageBR (10.7.2016)

[20] C.N. Yang, *Selection Rules for the Dematerialization of a Particle into Two Photons*, Phys. Rev. 77, 242, January 1950

[21] G. Aad et al. (ATLAS Collaboration), *Evidence for the spin-0 nature of the Higgs boson using ATLAS data*, Physics Letters B, Volume 726, Issues 1–3, 7 October 2013, Pages 120–144.

[22] J. C. Collins, D. E. Soper, Angular distribution of dileptons in high-energy hadron collisions, Phys. Rev. D16 (1977) 2219–2225.

[23] Adam Falkowski (2013-02-27). *When shall we call it Higgs?*, Résonaances particle physics blog, retrieved 7 March 2013.

[24] CMS Collaboration, Combination of SM Higgs Searches, http://cdsweb.cern.ch/record/1406347/files/HIG-11-032-pas.pdf, retrieved April 14 2016.

Leopold-Franzens-Universität Innsbruck

Eidesstattliche Erklärung

Ich erkläre hiermit an Eides statt durch meine eigenhändige Unterschrift, dass ich die vorliegende Arbeit selbständig verfasst und keine anderen als die angegebenen Quellen und Hilfsmittel verwendet habe. Alle Stellen, die wörtlich oder inhaltlich den angegebenen Quellen entnommen wurden, sind als solche kenntlich gemacht.

Ich erkläre mich mit der Archivierung der vorliegenden Bachelorarbeit einverstanden.

1. August 2016	
Datum	Unterschrift